Journal of Structural Geology 34 (2012) 54–60

Contents lists available at SciVerse ScienceDirect

Journal of Structural Geology

journal homepage: www.elsevier.com/locate/jsg

Anisotropy of magnetic susceptibility (AMS) and diamagnetic fabrics in the Durness Limestone, NW Scotland

G.J. Borradaile [a,*], B.S.G. Almqvist [b], I. Geneviciene [a]

[a] Lakehead University, Faculty of Science, Geology & Physics Department, 955 Oliver Road, Thunder Bay, ON P7B 5E1, Canada
[b] ETH Zurich, Geological Institute, 8092 Zurich, Switzerland

ARTICLE INFO

Article history:
Received 1 August 2011
Received in revised form
16 October 2011
Accepted 30 October 2011
Available online 9 November 2011

Keywords:
AMS
Diamagnetic
Blended fabric
"Inverse" fabric
Axis-switching
Paramagnetic-compatible

ABSTRACT

AMS fabrics in the Durness limestone show principal axes with orientations that are counterintuitive to, but symmetrical, with the regional tectonic axes (*X, Y, Z*) where *X* is the stretching axis and *Z* is the shortening axis. In the field, cleavage (*XY*) is nearly NS and nearly vertical. Low-field susceptibility measurements of 57 cores with positive bulk susceptibility ($\kappa > 0$) have a nearly vertical maximum susceptibility (κ_{MAx}) that is similarly oriented to the regional extension axis (*X*) but with intermediate susceptibility approximately parallel to the regional EW shortening axis. We explain this fabric as the blending of an oblate subhorizontal bedding with a north–south feeble tectonic AMS fabric, parallel to the regional N–S vertical cleavage. The 79 diamagnetic ($\kappa < 0$) cores reveal a similar AMS fabric when the orientations of the maximum and minimum axes are exchanged to produce a *paramagnetic-compatible* fabric.

1. Introduction and goal

The Durness Limestone mostly crops out as a weakly deformed carbonate forming part of the Cambro-Ordovician strata that overlie the basement of Proterozoic Torridonian sandstone and Lewisian gneiss in NW Scotland (Fig. 1a, b). For the most part the Durness limestone is a misnomer; it is commonly a dolostone formed in several episodes of early dolomitization and silicification (Park et al., 2002; Swett, 1969). It occurs in two major areas, repeated by faulting, one running NNE-SSW through the village of Durness and the other running along the east shore of Loch Eriboll (Fig. 1a), both west of and underlying the Moine thrust. The Moine thrust has an age not greater than 430 Ma (Goodenough et al., 2006) and the Moine schists are of late Proterozoic age (Kirkland et al., 2008), metamorphosed in the Silurian (Miller, 1961).

Most bedding planes in the Durness Limestone dip gently to the SE (Fig. 1c) and deformation is manifest by mostly irregular jointing and by a vertical N–S fracture and stylolitic cleavage (Fig. 2). Stylolites occur parallel to bedding and more rarely in a steep north-south orientation defining the cleavage. The latter are only visible in suitably weathered outcrops, mainly near the sea. Open folds are extremely rare and confined to the Loch Eriboll area where they verge toward the west or WNW (Fig. 2b). Unsuitable cores with too weak susceptibility constituted 30% of the total and they were excluded from further study, leaving 136 cores with suitably large *absolute* values for their bulk susceptibility. Sampling sites with successful block samples were evenly distributed with 28 sites located NNE-SSW along the Durness outcrop (the east shore of the Kyle of Durness) (Fig. 1) and 16 sites distributed along the east shore of Loch Eriboll (Fig. 1) fault block, again in a NNE-SSW direction.

Our goal was to determine the cryptic magnetic fabric of these rocks, knowing that this presents special challenges in measurement and interpretation in carbonates due to their low susceptibilities (Owens and Rutter, 1978) and diamagnetic nature (Hrouda, 2004). In general, AMS fabrics may detect the weakest alignments of minerals and thus may reveal early, incipient tectonic fabrics. The technique is reproducible, fast and largely non-destructive of the specimens determining the mean orientation of mineral grains, as Hrouda (1982) first comprehensively explained. The interpretation of *magnitudes* of principal susceptibility axes is fraught with difficulty but their *orientations* may correspond in orientation to axes of strain or syncrystallization stress or other significant petrofabric orientations such as bedding (Borradaile and Jackson, 2010).

The negative susceptibility of calcite or dolomite rich specimens causes some further complications (Hrouda, 2004; Rochette, 1988).

* Corresponding author. Tel.: +1 807 683 0680.
E-mail addresses: troodos@tbaytel.net, borradaile@lakeheadu.ca (G.J. Borradaile), bjarne.almqvist@erdw.ethz.ch (B.S.G. Almqvist).

0191-8141/$ – see front matter © 2011 Elsevier Ltd. All rights reserved.
doi:10.1016/j.jsg.2011.10.008

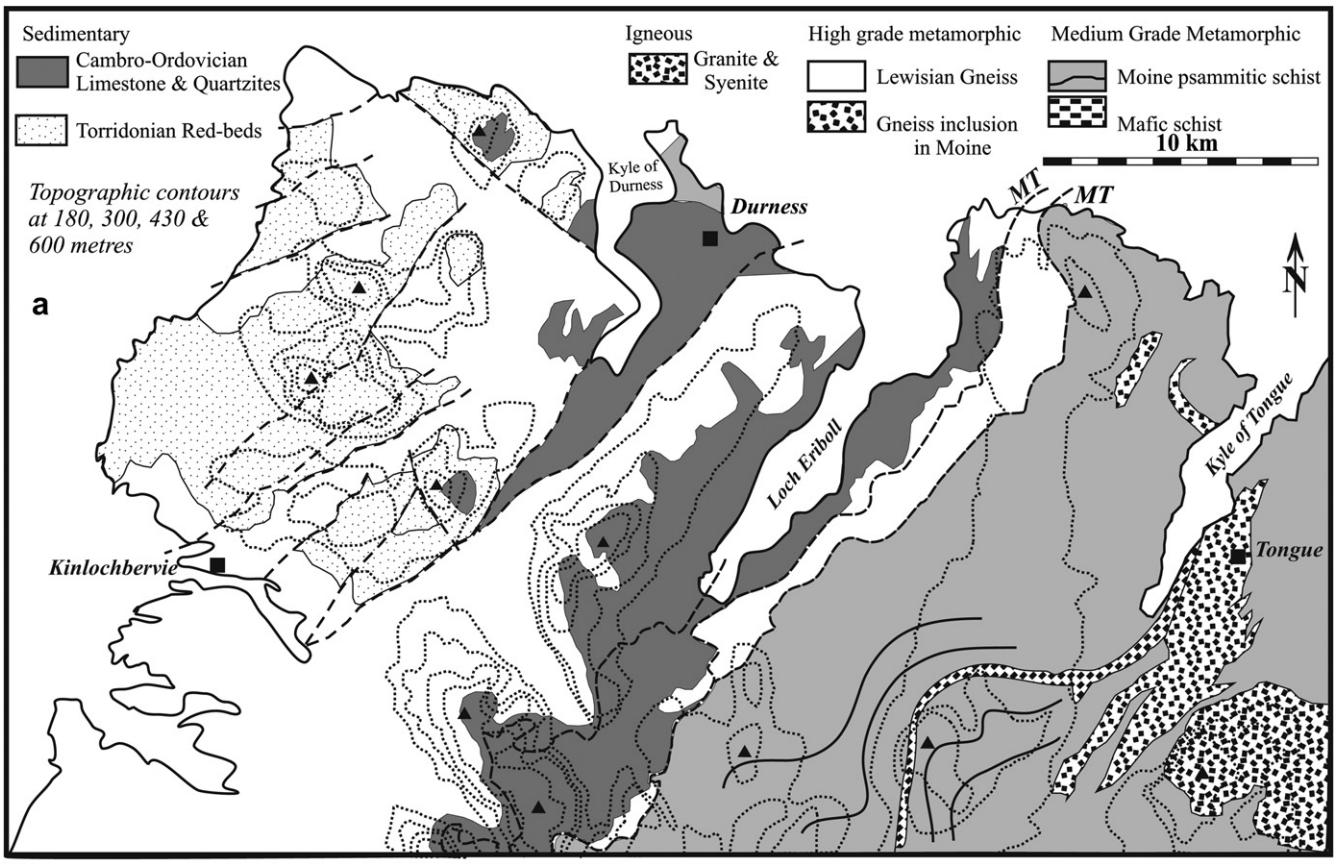

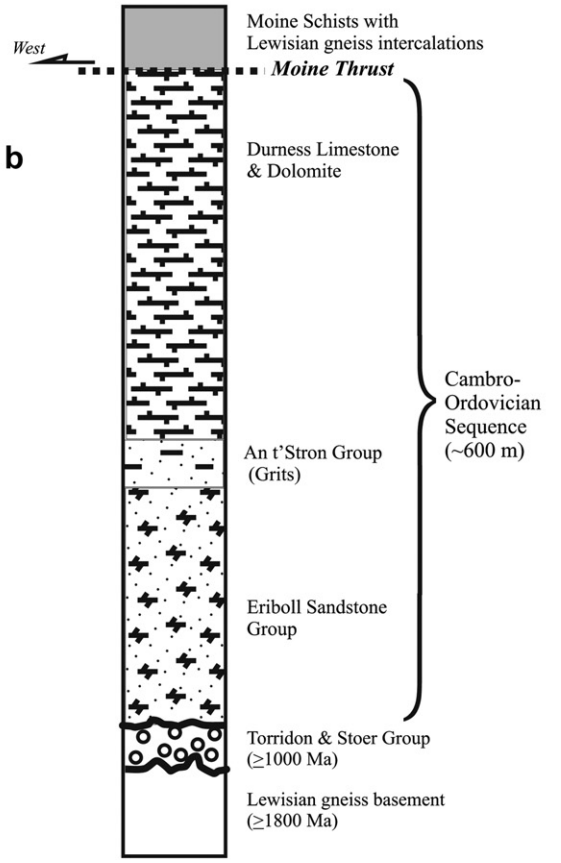

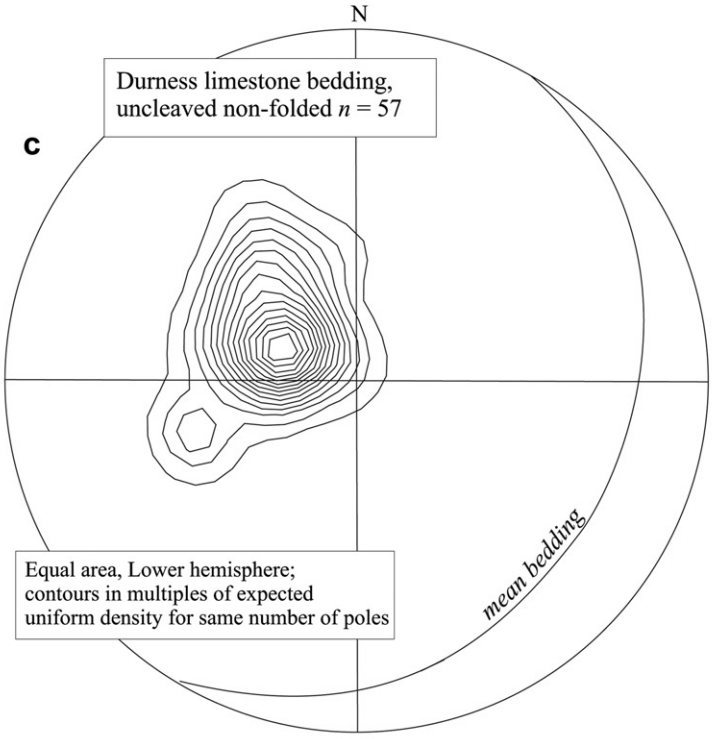

Fig. 1. Location, stratigraphy and plane-dipping structure of the Durness limestone.

Fig. 2. Durness limestone; (a) Plane-bedded, fractured and (b) rare folds.

The axis with the most negative magnitude aligns along the c-axis, which on petrofabric principles is parallel to the pole to tectonic schistosity. The literature commonly describes such a counterintuitive association of a susceptibility axis with a fabric axis (i.e., κ_{MAx}//Z) as an *inverse* fabric; this is relatively well known in the case of single domain magnetite (Potter and Stephenson, 1988). However, the use of "inverse" is more complicated in the case of diamagnetic carbonates (Hamilton et al., 2004; Rochette, 1988; Rochette et al., 1992; Schmidt et al., 2009; De Wall et al., 2000). Their most negative susceptibility aligns perpendicular to foliation (//Z). Here, to reduce confusion in the discussion of carbonate fabrics we avoid the use of "inverse" and refer instead to *diamagnetic fabrics*. For diamagnetic fabrics, the orientations of the maximum (most negative) and minimum (least negative) axes must be exchanged to produce *paramagnetic-compatible* fabrics. We will show that a steep, composite E–W magnetic diamagnetic foliation characterizes all the outcrops with $\kappa < 0$. Traces of magnetite are common in limestone from clastic, marine volcanic or bacterial origin and even permit paleomagnetic studies (Blakemore, 1975; Chang et al., 1987; Freeman, 1986) as in these rocks. Despite low concentrations, the magnetite may occasionally dominate the magnetic fabric because it cancels the diamagnetic susceptibility of the matrix in limestone giving rise to a net paramagnetic ($\kappa > 0$) response. The magnetic fabrics of those specimens are more directly interpretable.

Our paleomagnetic work in these carbonates produced ambiguous results of little paleomagnetic significance probably because our specimens possessed magnetizations that were too weak, unstable or affected by the tectonic petrofabric. However, carbonate breccia veins in the Durness limestone carry Triassic or Jurassic remanent magnetizations (Elmore et al., 2010). The same authors report characteristic remanent magnetizations of Devonian age from the limestone matrix, carried by magnetite and hematite and Elmore et al. (2003) reported Triassic magnetizations from non-deformed outcrops. These chemical or crystallization magnetizations (CRMs) are younger than the Durness group and postdate most alteration.

2. Magnetic properties

We studied magnetic fabrics using the anisotropy of magnetic susceptibility (AMS), in low-fields, which is challenging since most carbonates have near zero susceptibility. If pure, carbonate minerals are mostly diamagnetic, with a mean susceptibility $\kappa \leq -11$ μSI although their anisotropy is still easily measurable. However, Fe and Mg contents affect the diamagnetic susceptibility, contributing a paramagnetic component (Almqvist et al., 2010; Schmidt et al., 2007). Magnetite or clay trace impurities, with high positive susceptibility contaminated many specimens causing a near zero or low positive susceptibility. The susceptibility of magnetite is ~2.5 SI and clay minerals may have κ ~ 500 μSI,

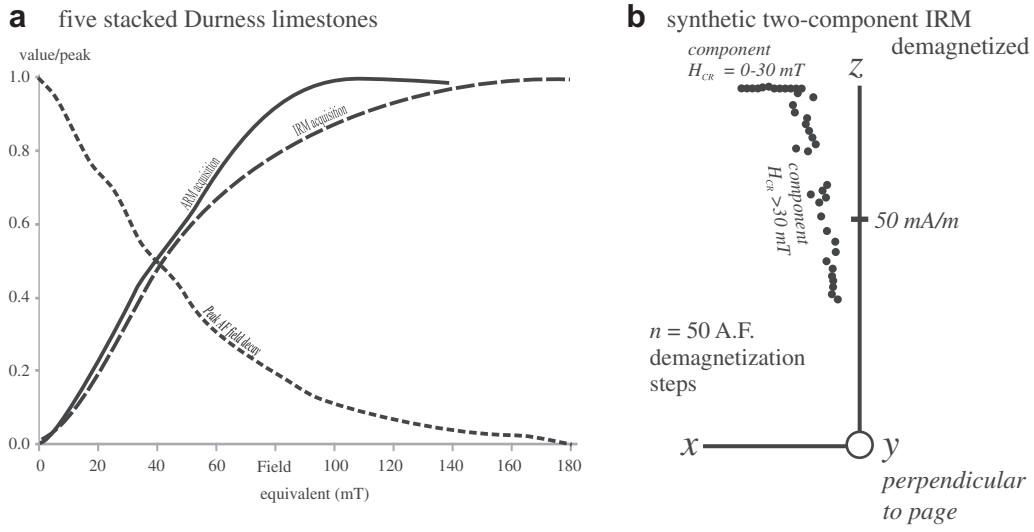

Fig. 3. (a) Acquisition and AF demagnetization of IRM, acquisition of ARM. (b) Progressive A.F. demagnetization of two orthogonal, synthetic IRM components.

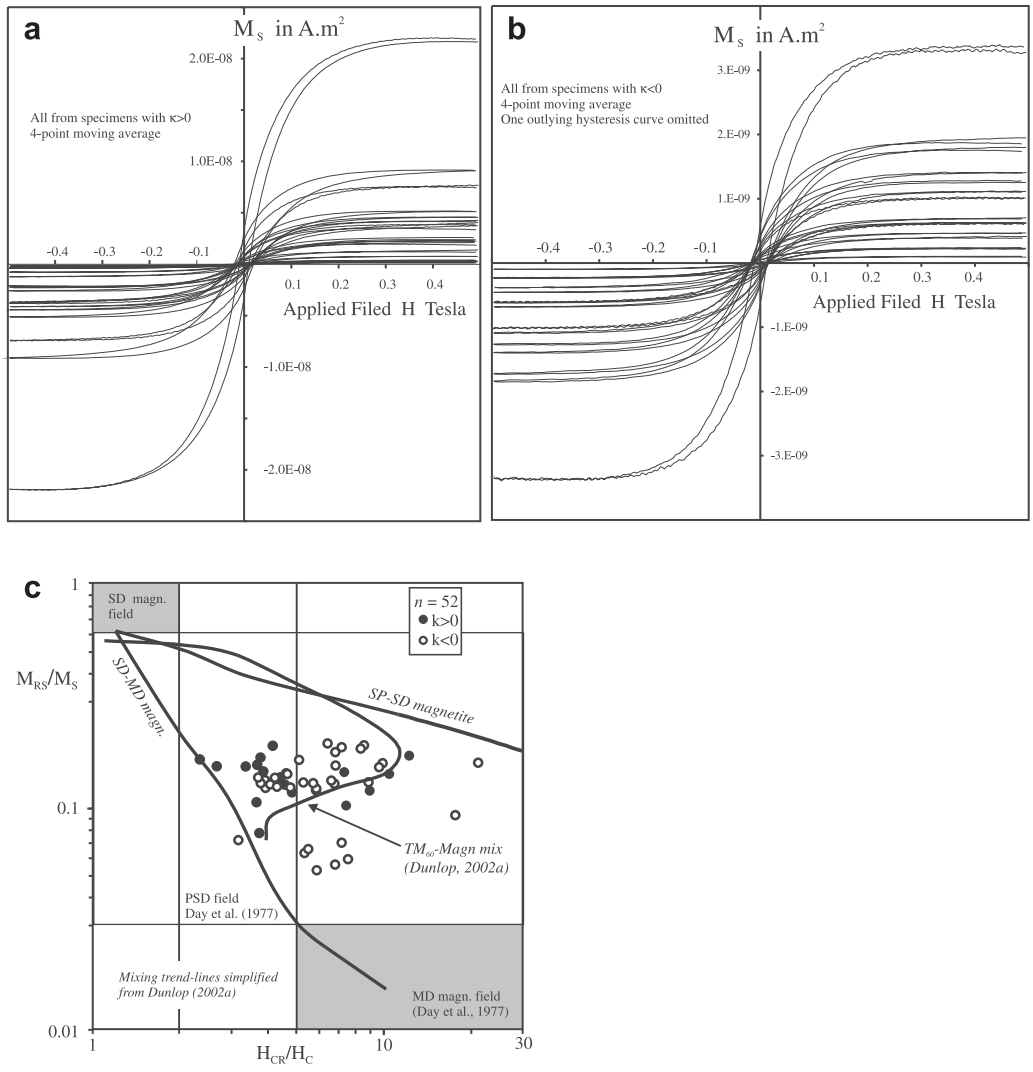

Fig. 4. Hysteresis data from Durness limestone using a Micromag2900 alternating force magnetometer. (a, b) Hysteresis loops, slope-corrected for the diamagnetic component so as to reveal the "ferro"-magnetic response. (c) Plot showing critical ratios that define magnetite domain-type response for our samples (after Day et al., 1977 with domain field boundaries from Dunlop, 2002). (H_{CR} = coercivity of remanence H_C = coercivity M_S = saturation magnetization M_{RS} = saturation remanent magnetization.).

whereas the susceptibility of calcite and dolomite are almost a million times smaller than magnetite. The anisotropy of specimens with bulk susceptibility near zero may be very difficult to measure since the differences between the magnitudes of the principal values (κ_{MAx}, κ_{INT}, and κ_{MIN}) may be close to the sensitivity of the measurement instrument or they may even vary in sign, which makes it impossible to calculate and anisotropy tensor. Furthermore, specimens with small absolute values for κ require very careful holder correction, a different value being required for each measurement-orientation. Holder cleanliness is also important since the susceptibility of paramagnetic dust can equal the anisotropic differences in susceptibility along different measurement-orientations through the specimen.

The presence of almost any other mineral may mask the negative (diamagnetic) susceptibility of carbonates ($\kappa \leq -11$ μSI). If clastic minerals are present in large numbers, for example in clay-rich limestone, the clay minerals and magnetite will dominate and the contribution of calcite to AMS will be negligible despite the fact that it forms the bulk of the rock. Any small contamination by paramagnetic or by remanence-bearing iron oxides may also complicate the interpretation of the fabric, e.g., the orientation of the principal susceptibility axes with respect to strain or petrofabric axes. We sampled 44 blocks of plane-bedded outcrops of Durness limestone, 28 from the Durness outcrops and 16 from the Eriboll outcrops (see Fig. 1a) and then laboratory-drilled four to six cores from each oriented block. We used a Sapphire Instruments SI2B instrument to determine low-field AMS, measuring susceptibility along seven differently oriented axes through the specimen using the algorithm of Borradaile and Stupavsky (1995).

High susceptibility traces of iron oxides are easily detectable since they may acquire and carry permanent or remanent magnetism. Thus, we studied their presence and nature from supplementary experiments in which we applied incrementally larger laboratory to produce isothermal remanent magnetizations (IRMs). We then removed the final, saturation IRM by alternating field (AF) incremental demagnetization to study the ease of demagnetization. Also, we applied anhysteretic remanent magnetization (ARM) to some other specimens since this is more comparable to a natural magnetization, although the ARM cannot be successfully demagnetized with the peak alternating field available to us (180 mT). Fig. 3 shows results for five specimens, stacked and averaged. The acquisition curves are typical of relatively small magnetite, behaving as pseudo-single domains (PSD). We verified this by applying two orthogonal synthetic IRM components. The first was

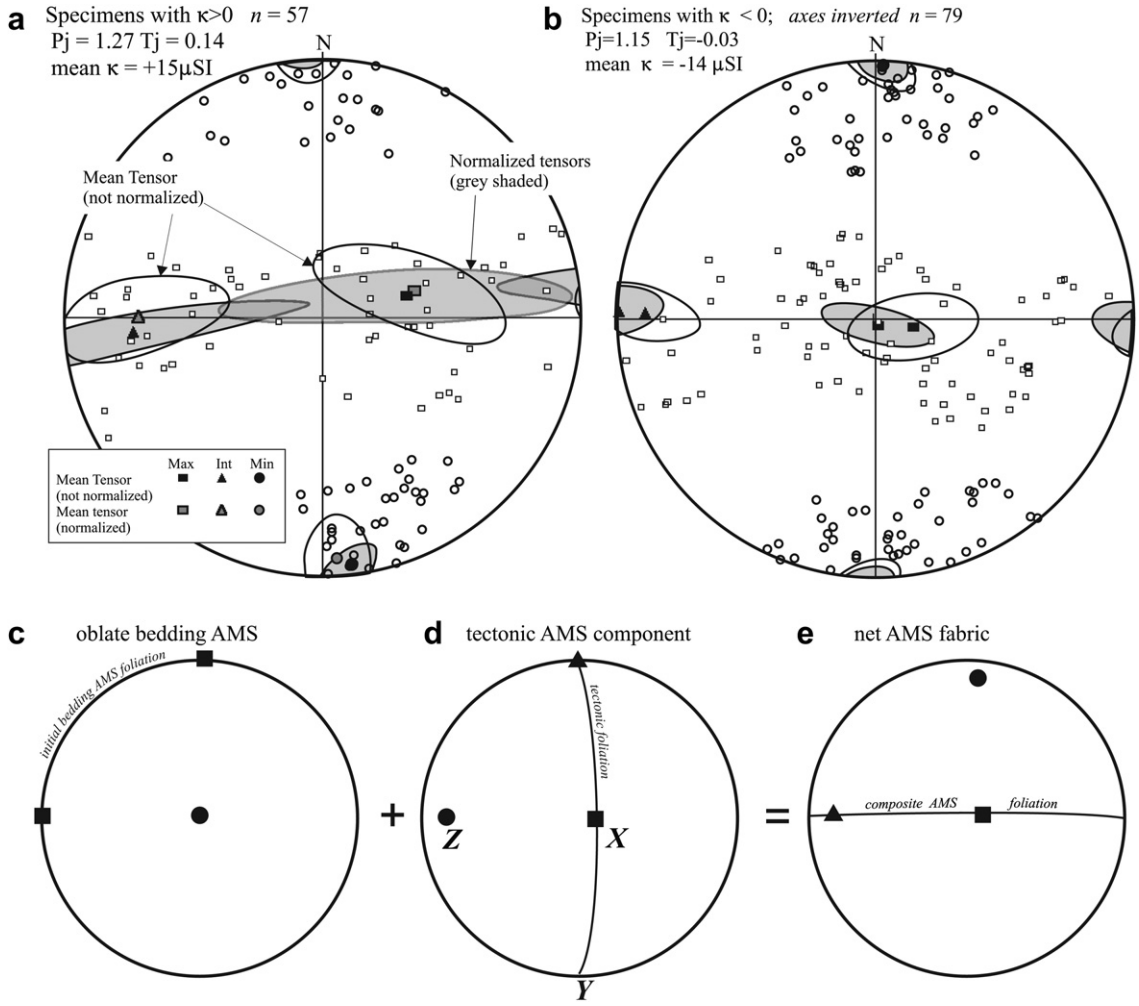

Fig. 5. (a) AMS axial orientations for Durness limestone, paramagnetic specimens. (b) Diamagnetic Durness limestone data. The axial orientations of the maximum and minimum axes have been exchanged to account for the diamagnetic nature of the fabric. This makes the data comparable to the paramagnetic specimens. Note apparent EW vertical magnetic "foliation" in both cases. Orientations are not slope-corrected for the dip of bedding, which dips gently SE (see Fig. 1c) and stereonets are equal area lower hemisphere. (c–e) for the paramagnetic case, this shows the proposed combination of primary and secondary fabrics that yield the composite final fabric. This is also valid for the diamagnetic case when maximum and minimum axes have been exchanged.

applied in a pulse magnetizer with a peak field of 500 mT along one axis. The specimen was than AF demagnetized along three axes to a peak field of 30 mT. Subsequently we applied a perpendicular IRM component in the pulse magnetizer with a peak field of 30 mT to magnetize the multi-domain (MD) magnetite. We then incrementally demagnetized the specimen to reveal the presence and relative importance of the two components carried by PSD-SD (>30 mT) and by MD (≤30 mT) coercivity grains (Fig. 3b). The failure to demagnetize the specimen completely may indicate the presence of hematite, which is of high coercivity.

We performed further experiments to determine hysteresis properties of the Durness specimens, using a Princeton Measurements Micromag2900 alternating gradient magnetometer (Fig. 4). Whether the specimens are dominantly diamagnetic ($\kappa < 0$) or have positive susceptibility, traces of PSD or SD magnetite are present in all specimens. We corrected the hysteresis loops for the slope of the diamagnetic (or paramagnetic) matrix component, so that the horizontal portions of the loops (Fig. 4a, b) define the saturation magnetization (Ms). The shape of the open part of the loop at low coercivity (applied fields < 100 mT) characterizes the "ferro"-magnetic response (Fig. 4a, b). Although elsewhere the Durness Limestone is hematized there is little evidence here of the higher coercivity that would be expected of hematite and, in this area, the limestone is dark gray in color. The ratios of hysteresis parameters (H_{CR}/H_C and M_{RS}/M_S) when plotted as axes of a Cartesian graph define fields that correspond to SD, PSD and MD magnetite (Day et al., 1977; Dunlop, 2002). The data scatter broadly in the PSD range, possibly toward the mixing line of titanomagnetite and magnetite (Dunlop, 2002) (Fig. 4c). This may indicate a submarine origin for the titanomagnetite since the characteristic source for TM_{60} ($Fe_{2.4}Ti_{0.6}O_4$) is ocean floor basalt.

3. Observations on magnetic fabrics (AMS)

The orientation of axes of magnetic susceptibility of the Durness Limestone shows a consistent pattern symmetrical with the regional tectonic scheme, but the axial magnitudes do not correspond simply to the regional strain axes. We should consider two items before plotting the axial orientations of the AMS ellipsoids. First, specimens with positive susceptibility plot in a simply interpreted fashion since maximum susceptibility (κ_{MAx}) has the tectonic significance of elongate fabric direction or net extension lineation (X) as in routine magnetic fabric investigations in high susceptibility tectonized rocks. Thus, for paramagnetic specimens, maximum susceptibility is steep and the intermediate susceptibility has a gentle westerly plunge (Fig. 5a), yielding an EW vertical

magnetic foliation. We interpret this in the usual fashion as a blending of an oblate bedding fabric with a feeble vertical tectonic one (Fig. 5c–e and see below).

Second, specimens dominated by the negative susceptibility of calcite or dolomite show a further complication due to the counterintuitive magnetic fabric in which the most negative susceptibility (with the largest absolute magnitude) has the tectonic significance of the shortening axis (Hrouda, 2004; Borradaile and Jackson, 2004). Therefore, in Fig. 5b, for the diamagnetic specimens, we exchanged the orientations of the κ_{MAx} and κ_{MIN} axes, producing a systematically comparable pattern to the specimens with positive susceptibility in Fig. 5a. The 95% confidence regions express the consistency and symmetry of the data. Although it makes relatively little difference here, we plotted the mean tensor axes both for the raw data, as well as for the specimens susceptibilities normalized by the bulk susceptibility (κ) (Fig. 5a, b; see Borradaile, 2001). The similarity between axes and confidence regions for the normalized and raw data suggests the petrofabric is relatively homogeneous without significant outliers of magnitudes or orientations.

4. Discussion of magnetic fabric

The significant question remains; why is the magnetic foliation (κ_{MAx}–κ_{INT}) is oriented vertically and East–West? One would expect the magnetic foliation to be steeply oriented but striking North–South, similar to the cleavage and axial planes of folds (Fig. 2). It is unlikely that the EW magnetic foliation has a direct petrofabric significance due to some unreported event of N–S shortening. Instead, we should consider the possibility of blended or mixed magnetic fabrics, where two magnetic subfabrics with differently oriented principal axes combine and conspire to produce a *composite* or net foliation (Borradaile and Tarling, 1981). More complex subfabric combinations may occur where normal and counter-intuitively oriented ("inverse" single domain or SD magnetite) fabrics overprint one another, as described by Ferré (2002) and Rochette et al. (1992). SD magnetite possesses a counterintuitive fabric since κ_{MAx} is parallel to its *short* axis (Potter and Stephenson, 1988) and if present in sufficient concentration it may counteract the contribution from intuitively oriented ("normal") mineral fabrics such as MD magnetite and paramagnetic silicates.

Grain dimensions control susceptibility axes in multi-domain magnetite but crystal symmetry dictates their orientation for pure rock-forming minerals. High symmetry rock-forming minerals (such as calcite) show a correlation of crystal and AMS axes but most rock-forming minerals are monoclinic or of lower symmetry so that their crystal habit and AMS ellipsoids are not coaxial (Borradaile and Jackson, 2010).

Furthermore, as previously mentioned, calcite, dolomite and quartz, being diamagnetic produce a counterintuitive effect since their largest magnitude susceptibility axis is the most negative (Hrouda, 2004; Rochette, 1988). It is parallel to the *c*-axis and on petrofabric grounds aligns with the pole to schistosity (Almqvist et al., 2009; Ihmlé et al., 1989; Hamilton et al., 2004). Subfabrics of different orientation may conspire to produce a variety of composite final axes. The combination of component subfabrics may be counterintuitive with respect to petrofabric axes in the case of calcite, dolomite or quartz. On the other hand, susceptibility axes may correspond to petrofabric axes (*normal* fabrics with $X//\kappa_{MAx}$, $Z//\kappa_{MIN}$) in the presence of paramagnetic and ferromagnetic minerals. The literature commonly refers to combinations of counterintuitive and normal fabrics as composite fabrics or "intermediate" fabrics. However, this may lead to confusion with "*intermediate axis* (κ_{INT}, or even *Y*)". Thus, here we use the terms *blended* or *composite* to describe a net fabric with any combination of subfabrics that yields a counterintuitive net fabric (e.g., Fig. 5c–e). A blended or composite fabric occurs wherever κ_{MAx} is not parallel to *X* and κ_{INT} is not parallel to *Y*. Fortunately, here as in many other cases of weakly strained sedimentary rock, the initial bedding fabric and the imposed tectonic subfabric are nearly orthogonal which simplifies the interpretations of axial orientations. Nevertheless, in detail, orientations of the composite susceptibility axes may not be easily predictable since they depend on the magnitudes of principal susceptibilities, and anisotropies (Pj, Tj values), of the component subfabrics.

From our measurements, the composite fabric is consistently oriented, resulting from the combination of the gently SE-inclined bedding fabric (Fig. 5c) with the N–S striking vertical tectonic foliation (Fig. 5d). Thus, we observe and a net East-West vertical

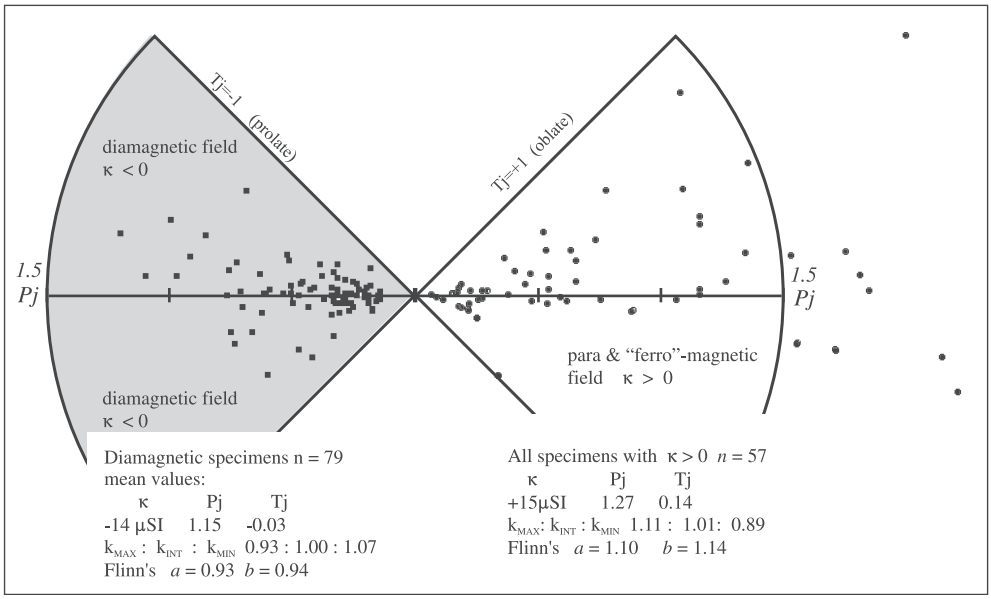

Fig. 6. Polar Pj–Tj plot of fabric shapes for Durness limestone. Note that most specimens have a neutral shape (Tj ~ 0) and the slight majority are diamagnetic (plotting left of origin).

composite magnetic foliation shown in Fig. 5e, with the data above in Fig. 5a, b. Fig. 5 shows AMS axes in geographic coordinates without a tilt correction for bedding.

The Pj and Tj parameters define fabric shapes and stretches of the AMS ellipsoid (Jelínek, 1981) (Fig. 6). Tj defines shape (+1 = oblate; −1 = prolate) and Pj defines the eccentricity or anisotropy degree of the ellipsoid ranging upward from a sphere (Pj = 0), comparable to the stretches of the strain ellipsoid. Since many of the specimens are diamagnetic, their fabric shapes with $\kappa < 0$ plot left of origin on the polar plot. Borradaile and Jackson (2004) explain several advantages of the polar plot over a Cartesian plot of Pj–Tj. The polar plot of fabric shapes (Fig. 6) shows that the fabrics plot mostly along a neutral shape-line (Tj ~ 1). Specimens with $\kappa > 0$ tend to show more oblate fabrics, possibly due to the presence of clay minerals or a foliation of fine magnetite.

5. Conclusions

The orientations of the magnetic fabrics define an E–W magnetic foliation with κ_{MAx} (vertical) and κ_{INT} (EW) (Fig. 5a,b). This petrofabric could be due to some separate microfabric-forming event, for example associated with the E–W vertical veining or N–S shortening. However, there is no other evidence for this and the AMS samples a fine-grained magnetic petrofabric within the limestone matrix. Thus, we tentatively interpret the E–W vertical foliation as a composite of the E–W shortening (Z) fabric observed in the field combined with the weak bedding-oblate fabric (Fig. 5c–e). The paramagnetic case is readily understood but the argument is also valid for the diamagnetic case when the orientations of the maximum and minimum axes are exchanged, to remove the counterintuitive effects of the diamagnetic fabric, producing a *paramagnetic-compatible* fabric (Fig. 5b).

Blended fabrics have orientations of the net or composite principal axes that do not correspond to the expected strain axes ($X \geq Y \geq Z$). This is complicated further by counterintuitive fabrics due to SD magnetite or to a diamagnetic matrix mineral. The permutations of composite (final) susceptibility axes vary, depending on the susceptibility-magnitude of each of the combined subfabrics, and on their orientation (Fig. 5c–e). Ferré (2002) and Rochette et al. (1992) discuss more of the possible permutations of composite axial orientations and magnitudes. Fortunately, weakly strained rocks present a simple situation because an oblate bedding subfabric will usually be nearly orthogonal to a superimposed tectonic subfabric. Moreover, usually one or both fabrics have κ of the same sign and both magnetic fabrics will be intuitively oriented with respect to petrofabric axes. Here the diamagnetic nature of the rocks complicated matters requiring careful consideration of the signs and magnitudes of principal susceptibility axes (Hrouda, 2004; Rochette, 1988; Hamilton et al., 2004). Nevertheless, the essence is that of subfabric mixing (Rochette et al., 1992), albeit of two counterintuitive diamagnetic subfabric components.

Acknowledgements

The authors are indebted to Mike Jackson and Doug Elmore for providing constructive reviews. NSERC (Ottawa, Canada) has supported Borradaile's research since 1979, for which we are indebted. Anne Hammond provided excellent drill core from the sampled blocks.

References

Almqvist, B.S.G., Hirt, A.M., Schmidt, V., Dietrich, D., 2009. Magnetic fabrics of the Morcles Nappe. Tectonophysics 466, 89–100. doi:10.1016/j.tecto.2008.07.014.

Almqvist, B.S.G., Herwegh, M., Schmidt, V., Pettke, T., Hirt, A.M., 2010. Magnetic susceptibility as a tool to study deformed calcite with variable impurity content. Geochemistry Geophysics Geosystems (G^3) 11, 1–15. doi: 10.1029/2009GC002900.

Blakemore, R.P., 1975. Magnetotactic bacteria. Science 190, 377–379.

Borradaile, G.J., 2001. Magnetic fabrics and petrofabrics: their orientation distributions and anisotropies. Journal of Structural Geology 23, 1581–1596.

Borradaile, G.J., Stupavsky, M., 1995. Anisotropy of magnetic susceptibility: measurement schemes. Geophysical Research Letters 22, 1957–1960.

Borradaile, G.J., Jackson, M., 2004. Anisotropy of magnetic susceptibility (AMS): magnetic petrofabrics of deformed rocks. In: Martin-Hernandez, F., Lünenburg, C.M., Aubourg, C., Jackson, M. (Eds.), Magnetic Fabric: Methods and Applications, vol. 238. Geological Society London, pp. 299–360. Special Publication.

Borradaile, G.J., Jackson, M., 2010. Structural geology, petrofabrics and magnetic fabrics (AMS, AARM, AIRM). Journal of Structural Geology 32, 1519–1551. doi:10.1016/j.jsg.2009.09.006.

Borradaile, G.J., Tarling, D.H., 1981. The influence of deformation mechanisms on magnetic fabrics in weakly deformed rocks. Tectonophysics 77, 151–168.

Chang, S.-B.R., Kirschvink, J.L., Stolz, J.F., 1987. Biogenic magnetite as a primary remanence carrier in limestone deposits. Physics of the Earth and Planetary Interiors 46, 289–303.

Day, R., Fuller, M., Schmidt, V.A., 1977. Hysteresis properties of titanomagnetites: grain-size and compositional dependence. Physics of the Earth and Planetary Interiors 13, 260–266.

De Wall, H., Bestmann, M., Ullemeyer, K., 2000. Anisotropy of diamagnetic susceptibility in Thassos marble: a comparison between measured and modelled data. Journal of Structural Geology 22, 1761–1771.

Dunlop, D.J., 2002. Theory and application of the Day Plot (M_{RS}/M_S versus H_{CR}/H_C). 1. Theoretical curves using titanomagnetite data. Journal of Geophysical Research 107 doi: 10.1029/2001JB000486.

Elmore, R.D., Blumstein, R., Engel, M., Parnell, J., 2003. Palaeomagnetic dating of fluid flow events along the Moine thrust fault, Scotland. Journal of Geochemical Exploration 78–79, 45–49. doi: 10.1016/S0375-6742(03)00069-4.

Elmore, R.D., Burr, R., Engel, M., Parnell, J., 2010. Paleomagnetic dating of fracturing using breccia veins in Durness group carbonates, NW Scotland. Journal of Structural Geology 32, 1933–1942. doi:10.1016/j.jsg.2010.05.011.

Ferré, E.C., 2002. Theoretical models of intermediate and inverse AMS fabrics. Geophysical Research Letters 29, 1–4. 31doi: 10.1029/2001GL014367.

Freeman, R., 1986. Magnetic mineralogy of pelagic limestones. Geophysical Journal of the Royal Astronomical Society 85, 433–452.

Goodenough, K., Evans, J., Krabbendam, M., 2006. Constraining the maximum age of movements in the Moine thrust belt: dating the Canisp Porphry. Scottish Journal of Geology 42, 77–81. doi: 10.1144/0036-9276/01-307.

Hamilton, T.D., Borradaile, G.J., Lagroix, F., 2004. Sub-fabric identification by standardization of AMS: an example of inferred neotectonic structures from Cyprus. In: Martin-Hernandez, F., Lünenburg, C.M., Aubourg, C., Jackson, M. (Eds.), Magnetic Fabric: Methods and Applications, vol. 238. Geological Society London, pp. 527–540. Special Publication.

Hrouda, F., 1982. Magnetic anisotropy of rocks and its application in geology and geophysics. Geophysical Surveys 5, 37–82.

Hrouda, F., 2004. Problems in interpreting AMS parameters in diamagnetic rocks, 49–59. In: Martin-Hernandez, F., Luneburg, C.M., Aubourg, C., Jackson, M. (Eds.), Magnetic Fabrics. Geological Society, London, pp. 49–60. Special Publ. No. 238.

Ihmlé, P.F., Hirt, A.M., Lowrie, W., Dietrich, D., 1989. Inverse fabric in deformed limestones of the Morcles Nappe, Switzerland. Geophysical Research Letters 16, 1383–1386.

Jelínek, V., 1981. Characterization of the magnetic fabrics of rocks. Tectonophysics 79, T63–T67.

Kirkland, C., Strachan, R., Prave, A., 2008. Detrital zircon signature of the Moine Supergroup, Scotland: contrasts and comparisons with other Neoproterozoic successions within the circum-North Atlantic region. Precambrian Research 163, 332–350.

Miller, J.A., 1961. Age of metamorphism of Moine schists. Geological Magazine 98, 85–86.

Owens, W.H., Rutter, E.H., 1978. The development of magnetic susceptibility anisotropy through crystallographic preferred orientation in a calcite rock. Physics of the Earth and Planetary Interiors 16, 215–222.

Park, R.G., Stewart, A.D., Wright, R.D., 2002. The Hebridean Terrain. In: Trewin, N.H. (Ed.), The Geology of Scotland, vol. 156. Geological Society of London Memoir, p. 576.

Potter, D.K., Stephenson, A., 1988. Single-domain particles in rocks and magnetic fabric analysis. Geophysical Research Letters 15, 1097–1100.

Rochette, P., 1988. Inverse magnetic fabric in carbonate-bearing rocks. Earth and Planetary Science Letters 90, 229–237.

Rochette, P., Jackson, M.J., Aubourg, C., 1992. Rock magnetism and the interpretation of anisotropy of magnetic susceptibility. Reviews of Geophysics 30, 209–226.

Schmidt, V., Hirt, A.M., Hametner, K., Günther, D., 2007. Magnetic anisotropy of carbonate minerals at room temperature and 77K. American Mineralogist 92, 1673–1684.

Schmidt, V., Hirt, A.M., Leis, B., Burlini, L., Walter, J.M., 2009. Quantitative correlation of texture and magnetic anisotropy of compacted calcite-muscovite aggregates. Journal of Structural Geology 31, 1062–1073.

Swett, K., 1969. Interpretation of Depositional and Diagenetic History of Cambrian-Ordovician Succession of Northwest Scotland. Northwestern Border of the Orogenic Belt. AAPG Special Volume M12, vol. 45. Geology and Continental Drift, North Atlantic. Chapter 630–646.